

# Critical current in Nb-Cu-Nb junctions with non-ideal interfaces

Y. Blum<sup>1</sup>, A. Tsukernik<sup>2</sup>, M. Karpovski<sup>1</sup>, A. Palevski<sup>1</sup>

<sup>1</sup> School of Physics and Astronomy, Tel Aviv University, Tel Aviv 69978, Israel

<sup>2</sup> University Research Institute for Nanoscience and Nanotechnology, Tel Aviv University, Tel Aviv 69978, Israel

We report on experimental studies of superconductor (Nb) -normal metal (Cu) -superconductor (Nb) junctions with dirty interfaces between the different materials. By using a set of simultaneously prepared samples, we investigated the thickness dependence as well as the temperature dependence of the critical currents in the junctions. Good agreement between the decay of the measured critical currents and theoretical calculations was obtained without any fitting parameters.

## I. INTRODUCTION

The non-dissipative current, as well as other superconducting properties, are induced in the normal metal by an electron-hole pair that is formed during the Andreev reflection at the superconductor (S) -normal metal (N) interface<sup>1</sup>. The finite length over which the electron-hole pair remains correlated determines the characteristic decay length,  $\xi_N$ , of the superconducting current in SNS junctions. The normal-metal thickness,  $L$ , and temperature dependence of the super-current in the long SNS junctions,  $L > \xi_N$ , has been thoroughly investigated over the last few decades, both theoretically<sup>2-4</sup> and experimentally<sup>5-7</sup>.

However, only in the case of junctions with clean interfaces, was reasonably good agreement between the theory<sup>2</sup> and the experiment<sup>7</sup> found. In practice, there is no way to produce vanishing boundary resistance. Nevertheless, the ratio of the latter to the resistance of the normal metal in the junction could be made much smaller than unity, as was the case for the lateral junctions in Ref. 7. In this limit, the theories developed for the ideal interface junction are valid. It should be emphasized, that the high quality interface obtained during *in situ* sequential deposition of two materials could result in large values of the ratio provided that the resistance of the normal-metal in the junction attains a low value. For non-ideal junctions, namely, for devices with vertical junctions, the ratio of interface to normal-metal resistances is usually larger than unity. Therefore, for such devices the theory of the ideal interface limit<sup>2</sup> is not applicable. The influence of boundary scattering on the critical current in SNS junctions has been considered theoretically in the past<sup>3,4</sup>. However, so far, there is no experimental data which quantitatively verifies the theoretical prediction. The most remarkable difference between the theoretical predictions for the ideal and non-ideal junctions is reflected in the dependence of the critical superconducting current,  $I_C$ , on the total junction resistance in the normal state,  $R_j$ . For the ideal junctions, where normal-metal resistance is the main contributor to the total  $R_j$ ,  $I_C \propto R_j^{-1}$ . In the opposite limit, where the main contribution to  $R_j$  arises from the interface resistance, the super-current is proportional to  $R_j^{-2}$ .

This paper is devoted to experimental studies of the critical current in vertical Nb-Cu-Nb long junctions with

a large ratio of interface to normal-metal resistances. We demonstrate good quantitative agreement with the theory of Kupriyanov *et al.*<sup>4</sup> in the appropriate limit.

## II. THEORETICAL BACKGROUND

For the long SNS junction, the one dimensional Usadel equations<sup>8</sup> are used with the appropriate boundary conditions. In the zero approximation in the Matsubara frequencies, the critical current in a junction with ideal interfaces can be expressed as follows<sup>2</sup>:

$$I_c = \frac{64\pi k_B T}{e R_j} \frac{\Delta^2(T)}{[\pi k_B T + \Omega + (2\Omega(\pi k_B T + \Omega))^{1/2}]^2} \frac{L}{\xi_N} e^{-\frac{L}{\xi_N}} \quad (1)$$

where  $\Delta(T)$  is the superconductor energy gap,  $\Omega = \sqrt{(\pi k_B T)^2 + \Delta^2(T)}$ , and  $\xi_N = \sqrt{\frac{\hbar D}{2\pi k_B T}}$  the thermal length.

In the case of non-ideal interfaces (transmission less than unity) between the normal metal and superconductors, the Eilenberger equations<sup>9</sup> must first be solved for the vicinity of the boundary, after which it is possible to write the boundary conditions for the Usadel equations.

Following Ref. 4, the resistivity of the structure in the normal state can be expressed as

$$R_j = \frac{L}{\sigma_N A} (1 + 2\Gamma_B) \quad (2)$$

where  $\sigma_N$  is the normal metal conductivity, and  $\Gamma_B = \frac{\xi_N \gamma_B}{L}$ . Here,  $\gamma_B$  is a parameter related to the transparency of the interface.

In the limit of SN boundary with small transparency  $\gamma_B \gg (\frac{T_c}{T})^{1/2}$ , the critical current in the first order of the Matsubara frequency is given by<sup>4</sup>:

$$I_c = \frac{4\pi k_B T_c}{e R_j} \frac{1 + 2\Gamma_B}{\gamma_B^2} \frac{\Delta^2(T)}{(\pi k_B T)^2 + \Delta^2(T)} \frac{L}{\xi_N} e^{-\frac{L}{\xi_N}} \quad (3)$$

where  $T_c$  is the superconductor critical temperature. For the low transparency junctions, namely  $\Gamma_B \gg 1$ , the critical current can be expressed in terms of measurable quantities as follows:

$$I_c = \frac{16\pi k_B T_c \rho_N}{e A_j R_j^2} \frac{\Delta^2(T)}{(\pi k_B T)^2 + \Delta^2(T)} \frac{\xi_N^{*2}}{\xi_N} e^{-\frac{L}{\xi_N}} \quad (4)$$

where  $\rho_N$  is the normal metal resistivity and  $\xi_N^* = \sqrt{\frac{\hbar D}{2\pi k_B T_c}}$ . Eq. 4 is valid only for  $L \gg \xi_N$ . For  $L \geq \xi_N$  the contribution of higher harmonics of the Matsubara frequencies should be included (see Eq. (34) of Ref. 4).

### III. SAMPLE PREPARATION AND MEASUREMENT SET-UP

The samples were fabricated as long triangular prisms. Two SNS junctions were created along the prism in a SQUID like geometry as shown schematically in Fig.1. This design allows the observation of Little-Parks oscillations<sup>10</sup> which give two advantages. First, it is possible to ensure zero magnetic flux through the junctions. Second, accurate measurements of the normal resistance and the cross section area of the junctions is possible.

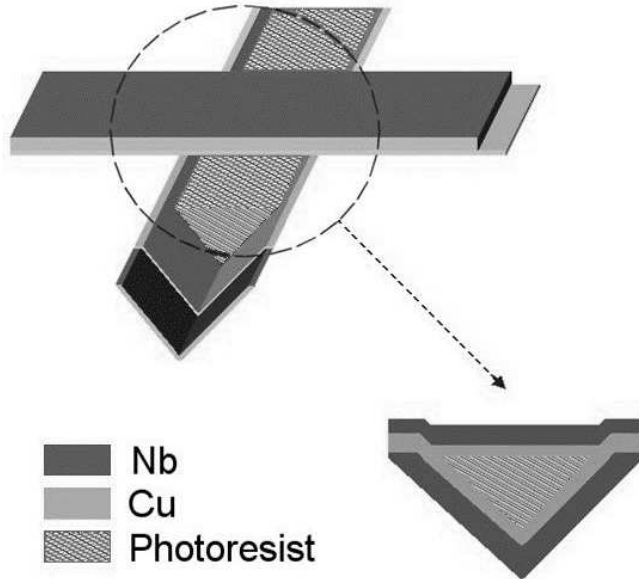


FIG. 1. Schematic drawing of a sample. A cross section of the structure is given on the right side.

The SNS junctions were fabricated on top of V-shaped substrates, produced by wet-chemical crystallographic etching<sup>11</sup> of GaAs planar substrates.

The V-groove substrate was covered with Nb and Cu films, which produced the two bottom side-walls of the prism. Nb films were sputtered using a magnetron gun and covered *in situ* with a Cu layer by thermal evaporation, to prevent Nb oxidation. An additional Cu layer was e-gun evaporated in a separate vacuum chamber. These layers were completely covered by photoresist. Oxygen plasma etching was applied in order to expose the top parts of the V-groove. The subsequent depositions of the Cu and Nb films, as described above, completed the fabrication of the prism samples. The crossing geometry

of the top and the bottom films allowed four terminal measurement of the junction below the critical temperature of the Nb films.

Nine sets of samples were prepared simultaneously in order to assure identical interfaces at all junctions. The samples of each set had an identically thick Cu layer. Variation of the Cu layer thickness between the different sets was obtained by a specially designed shutter, which exposed the samples in sequence, so that every set was exposed to the evaporating Cu for additional fragments of time. Thus, the only difference between the sets was the thickness of the Cu layer. We prepared separate Cu films simultaneously with the deposition of the Cu in the junctions. The measured resistivity of these Cu films at 4.2K was  $\rho_N = 5.5 \cdot 10^{-9} \Omega m$ .

The thickness of each Nb layer was  $2000 \text{ \AA}$ , whereas the Cu thickness varied from  $L = 2000 \text{ \AA}$  to  $L = 10000 \text{ \AA}$ . The area of the junction,  $A_j$ , relevant for the critical current is determined by the width of the Nb strips,  $W_{Nb} = 10 \mu m$ , and the width of the exposed top part of the V-groove,  $W_{top}$ . The cross-section of the junction relevant for the flux dependence of the critical current in the junction is given by  $LW_{top}$ . The overall flux dependence of the critical current in the SQUID sample is determined both by the area of the junction and the total cross section of the SQUID ( $A_{SQUID} = 6.5 \mu m^2$ ), as given in the following expression<sup>12</sup>:

$$I_{c_{total}} = 2I_{c_j} \left| \cos \frac{\pi \Phi}{\Phi_0} \left[ \frac{\sin(\pi \Phi_j / \Phi_0)}{\pi \Phi_j / \Phi_0} \right] \right| \quad (5)$$

where  $I_{c_j}$  is the critical current of one junction, while  $\Phi$  and  $\Phi_j$  are the flux in the SQUID and junction respectively.

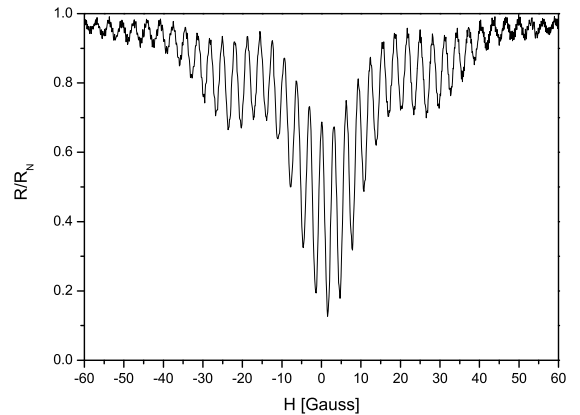


FIG. 2. Typical magnetoresistance plot as measured in a sample with a layer of  $8000 \text{ \AA} \text{ Cu}$ .

The measurements were performed in a  $^4\text{He}$  cryostat in the range 1.3K-4.2K. The critical current was measured by passing a DC current with a small AC modulation through the sample. The AC voltage, which appeared above the critical DC current, was picked up by a lock-in amplifier operated in transformer mode.

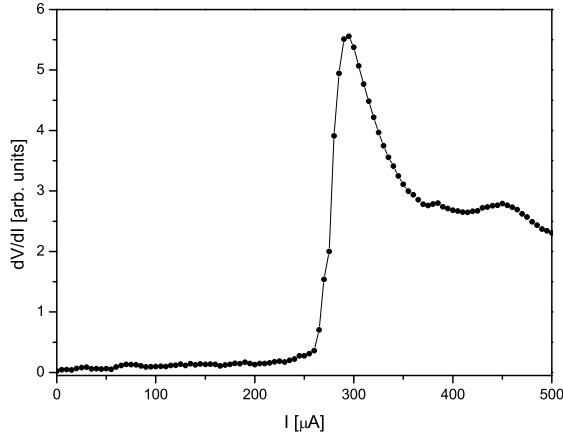


FIG. 3. Typical variation of the differential resistance of a SNS junction. The onset of the peak was defined as the critical current of the junction.

#### IV. EXPERIMENTAL DATA AND ANALYSIS

We start the description of our data with the magnetoresistance oscillations of the samples. Fig.2 shows a typical magnetoresistance plot for a sample with a Cu thickness of  $L = 8000\text{\AA}$ . The short oscillation period,  $\Delta H = 3.1$  Gauss, corresponds to the area  $6.5\mu\text{m}^2$  enclosed by the SQUID, which is consistent with our designed geometry of the samples. The beating modulation with larger period and attenuation of the oscillations arises from additional Fraunhofer oscillations of the critical current in each junction (see Eq. 5), with typical area  $LW_{top}$ . Therefore, the analysis of the magnetoresistance oscillations allows us to extract  $W_{top} = 1.2\mu\text{m}$ , resulting in  $A_j = 12\mu\text{m}^2$ . Thus, magnetoresistance oscillations determine the geometrical dimensions of our samples, given in the previous section in the parenthesis.

The critical currents in our samples were measured at temperatures in the range of 1.3K-4.2K using the setup described above. A typical differential resistance of a sample vs. DC current is plotted in Fig.3, which clearly indicates the sharp onset of dissipation at  $I = I_c$ .

Some of the parameters which appear in Eq. 1 and Eq. 4, namely  $R_j = 19\text{m}\Omega$ ,  $T_c = 8.0\text{K}$  and  $\rho_{Cu} = 5.5 \cdot 10^{-9}\Omega\text{m}$ , are directly measured in our experiment. The rest of the parameters, namely  $\xi_N$ ,  $\xi_N^*$  and  $\Delta$  can be calculated. The diffusion coefficient, which appears in

$\xi_N$  and  $\xi_N^*$ , can be calculated from the measured resistivity of the Cu, using the relation  $D = (e^2 N(\epsilon_F) \rho)^{-1}$ , where  $N(\epsilon_F) = 1.56 \cdot 10^{47} \text{J}^{-1}$  is the density of states at the Fermi energy for Cu<sup>13</sup>. From the latter, we obtain  $D = 4.5 \cdot 10^{-2} \text{m}^2/\text{sec}$ . The energy gap is calculated using the known relation for Nb<sup>12</sup>  $\Delta = 1.9k_B T_c = 1.3\text{meV}$ . Thus, there are no free parameters entering the theoretical expressions.

We should keep in mind that Eq. 3 is only valid for large values of  $\gamma_B$ . The value of  $\gamma_B$  calculated from Eq.2 is about 500, and consequently,  $\Gamma_B$  varies between  $\sim 50$  for  $L = 9000\text{\AA}$  to  $\sim 200$  for  $L = 2000\text{\AA}$ . These values justify the applicability of both Eq.3 and Eq.4.

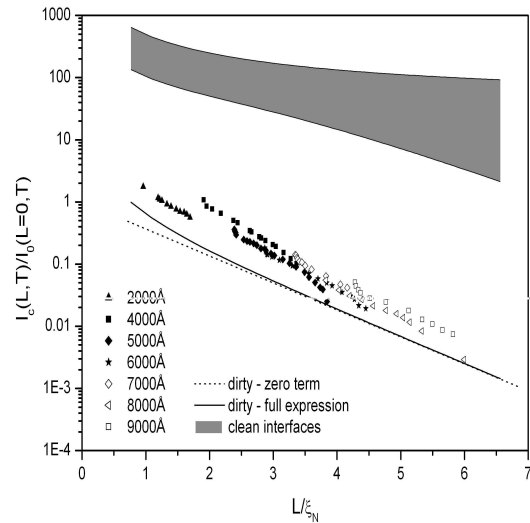


FIG. 4. Universal curve of the critical currents (dimensionless units), and the theoretical fits with the parameters described above. The dashed line represents Eq. 4, the solid line represents the infinite series (Eq. 34 in Ref. 4) and the gray area represents the theory for clean interface junctions<sup>2</sup> with thickness between  $2000\text{\AA}$  and  $9000\text{\AA}$ .

Since our aim is to compare our experimental data with the theory of Kupriyanov *et. al*<sup>4</sup>, we choose a dimensionless frame of axis  $(L/\xi_N, I_c(T, L)/I_0(T))$ , where  $I_0(T) = \frac{16\pi k_B T_c \rho_N}{eA R_j^2} \frac{\Delta^2(T)}{(\pi k_B T)^2 + \Delta^2(T)} \frac{\xi_N^*{}^2}{\xi_N}$ . These axes are natural for the  $I_c$  variation since the leading term in the Matsubara frequency expansion (Eq. 4) is just a simple exponential dependence, and therefore all our data points, presented in this frame of axis, should collapse onto a single exponential curve. Fig. 4 shows all our data points which quite closely follow (within a factor of two) the theory of Kupriyanof *et. al*. The dashed line in Fig. 4 corresponds to Eq. 4, while the solid line accounts for all Matsubara frequencies (Eq. 43 in Ref. 4).

The consistency with the latter theory is even more striking when the data is compared with the theory developed for a junction with clean interfaces<sup>2</sup>. Since for

this theory, the chosen frame of axis is not natural, our data should fall into the gray area. The upper border of the area corresponds to  $L = 2000\text{\AA}$  while the lower border corresponds to  $L = 9000\text{\AA}$ . Our data deviates by about three orders of magnitude from the theory of Zaikin *et al.*

It should be noted that there are no free parameters in the evaluation of the theoretical formula. The origin of the deviation of our data from the theoretical curve is not clear, and could arise from several sources. The estimate of the area from the Frounhofer oscillations has at least  $\pm 20\%$  error. The smaller area would increase  $I_0$  and therefore, improve the fit to the theory. The additional source of the error could arise from the value of  $\rho$  in the Cu layer. As explained above, it was determined from the resistivity measurement of the Cu film in the planar geometry. Although the small grain Cu films usually do not show significant anisotropy, one should bear in mind that the deposition of our Cu films was made with two interaptions (when moving the samples from the sputtering chamber to the e-gun deposition chamber and back). These additional interfaces with partially oxidized Cu could make the resistivity of the Cu very anisotropic, being much larger in the direction perpendicular to the interface than the measured values in planar geometry. We have no experimental way of verifying this. Apart from increasing  $I_0$ , and therefore improving the fit, the additional interfaces could make some non-trivial changes to the boundary conditions of the Usadel equations, which were not accounted for by the theory.

## V. CONCLUSIONS

We demonstrated that the theory<sup>4</sup> of the critical current in a SNS junction with non-ideal interfaces closely follows our experimental data. Keeping in mind that we have not used any fitting parameters, we find the agreement quite amazing. We claim that for vertical junctions with a clean normal-metal (even for those prepared *in situ*) the theory of Kupriyanov *et. al.*<sup>4</sup> is the relevant one. The theory developed for ideal-interface junctions<sup>2</sup> may

be applicable either for lateral junctions or for vertical junctions containing a strongly disordered metal, since only in these cases, the interface resistance could become negligible relative to the resistance of the normal metal.

## ACKNOWLEDGMENTS

We would like to thank A. Aharony, O. Entin-Wohlman, Y. Imry, K. Kikoin, Z. Ovadyahu, A. Schiller, G. Schön, K. Efetov and A. Gerber for fruitful discussions. This research was supported by a Grant from G.I.F., the German-Israeli Foundation for Scientific Research and Development as well as the Israel Science Foundation founded by the Israel Academy of Sciences and Humanities — Center of Excellence Program.

- 
- <sup>1</sup> A. F. Andreev, Sov. Phys. JETP 19, 1228 (1964).
  - <sup>2</sup> A. D. Zaikin, G. F. Zharkov, Fiz. Nizk. Temp. 7, 375 (1981) [Sov. J. Low Temp. Phys. **7**, 184 (1981)].
  - <sup>3</sup> M. Yu. Kupriyanov and V.F. Lukichev, Sov. J. Low Temp. Phys. **8**, 526 (1982).
  - <sup>4</sup> M. Yu. Kupriyanov and V.F. Lukichev, Sov. Phys. JETP **67**, 1163 (1988).
  - <sup>5</sup> J. Clarke, Proc. R. Soc. Lond. A 308, 447 (1969).
  - <sup>6</sup> H. Courtois, Ph. Gandit, B. Pannetier, Phys. Rev. B **52**, 1162 (1995).
  - <sup>7</sup> P. Dubos, H. Courtois, B. Pannetier, F.K. Wilhelm, A.D. Zaikin, G.Schön, Phys. Rev. B **63**, 64502 (2001).
  - <sup>8</sup> K.D. Usadel, Phys. Rev. Lett. **25**, 507 (1970).
  - <sup>9</sup> G. Eilenberger, Z. Phys. **214**, 195 (1968).
  - <sup>10</sup> W. A. Little, R. D. Parks, Phys. Rev. Lett. **9**, 9 (1962).
  - <sup>11</sup> A. Tsukernik, A. Palevski, V. J. Goldman, S. Luryi, E. Kapon, A. Rudra, Phys. Rev. B **63**, 153315 (2001).
  - <sup>12</sup> T. Van Duzer, C. W. Turner, “*Principles of Superconductive Devices and Circuits*” (Elsevier, New York, 1981).
  - <sup>13</sup> F. Pierre, A. B. Gougam, A. Anthore, H. Pothier, D. Esteve, N. O. Birge, Phys. Rev. B **68**, 85413 (2003).